Rapid Traversability Assessment in 2.5D Grid-based Map on Rough Terrain

Jiajun Gu, Qixin Cao and Yi Huang
Shanghai Jiaotong University
Research Institute of Robotics
Shanghai, China
kingjiajun@sjtu.edu.cn

Abstract: *This paper presents a rapid traversability assessment approach based on an extended 2.5D grid-based representaion of the rough terrain. Stereo vision system is used to perceive the environment surrounding robot. Conventional 2D, 3D and other 2.5D grid maps determine the traversability indices of the grids directly from the sensor feedback, while our approach attempts to address the indices of terrain from multiple grids instead. By analyzing the properties of multiple grids that the robot is to traverse, passable grids are distinguished, which also takes the robot's size into account. Fuzzy logic framework is applied to extract traversabiltiy indices from the terrain characteristics. A soccer robot equipped with a stereo vision system is adopted for experiments. The results show that our map is capable of speeding the process of traversability assessment and providing an autonomous mobile robot with a appropriate representation of 3D uneven terrain profile.*
Keywords: *outdoor environment, 2.5D grid, traversability index, fuzzy logic*

1. Introduction

Unmanned planetary exploration and operation on rough terrain have driven forwards research in autonomous navigation of mobile robots in recent years. Purely sensor-based navigation systems have been proven to be "short-sighted", since they simply react to the perception and do not reuse previous knowledge or estimate. For this reason, robot is usually equipped with a map which can represent its operating environment. The method to perceive and model the unkonwn environment is one of the key problems in building truly autonomous mobile robots. Robotic mapping is referred to as the process of generating spatial models of physical environments from sensor measurements through navigating in the environment (Huang, G.Q. ; Rad, A.B. & Wong, Y.K. 2006). In the past two decades, this field has received considerable attention and remarkable development has been achieved. Laser range finder (LRF) (Hähnel, D. ; Burgard, W. & Thrun, S. 2003) and stereo vision system (Murray, D. & Jennings, C. 1997) are widely used to acquire the environmental information during robot's operation. The two sensor systems both return rich information of environmental profile by means of dense point set. In recent years, stereo vision system is getting more and more attention in environmental modeling because of its high flexiblity and realibiltiy.

In order to maintain the environmental information perceived duiring robot's operation, grid-based maps (Touchton, B. et al 2006) are frequently adopted in autonomous navigation through tessellation of robot's configuration space. Diverse grid-based maps have been developed attempting to find a efficient solution to maintenance of environmental information. Occupancy grid map is proposed by Elfes, A. 1989 and is proven efficient by distinguishing obstacles from free areas (Habib & Maki, K. 2007). Such 2D grid-based maps assume that the robot operates in environment where the ground is flat and smooth, which make such type of grid maps usually found in indoor navigation. In exploration on rough terrain, however, the robot has to negotiate with the environment by circumventing impassable obstacles but traversing low-profile barriers as necessary. For example, the robot must be able to use its map to identify and move around steep ramps which might tip the robot over while identifying and traversing more gentle elevation changes. Moravec, H. P. (1996) proposed 3D evidence grid maps for outdoor environment. Gutmann, J.S. ; Fukuchi, M. & Fujita, M. (2005) present a 2.5D grid representation for indoor environment. This 2.5D grid map is used to distinguish stairs and obstacles from the traversable areas. Traversability index, firstly proposed by Seraji, H. (1999), is used to efficiently address terrain's ease-of-traverse for unmanned planetary exploration on Mars. This index is developed using the fiamework of fuzzy logic, and is expressed by linguistic fuzzy sets that quantify the suitability of the terrain for traversal based on its physical properties. Indices in research of Seraji, H. (1999) use terrain characteristics of slope and roughness, which are acquired by means of stereo vision. Liu, H. ; Yang, J. & Zhao, C. (2004) build fuzzy logic-based traversabilty indices from terrain properties of slope, roll variance and roughness. Ye, C. & Borenstein, J. (2004) employs laser range finder and identifies indices from

slope and roughness. Shirkhodaie, A. et al (2005) design three different traversability classifier for Mars surface according to three different soft computing techniques.

Based on existed types of grid maps, this paper aims to develop a novel 2.5D grid-based modeling method which can represent the outdoor environment incrementally and efficiently during robot's operation. Each grid contains the average height instead of the occupancy within the area that the grid patch represents. Unlike other grid maps, the grid size is determined by the size of robot's wheel instead of robot's body. Terrain characteristics like height difference, slope and roughness can be efficiently assessed from grids' average height instead of directly from dense sensor feedback from stereovision, which will speed the functions such as traverability assessment.

The rest of this paper is organized as follows. We will briefly review other grid-based modeling approaches and introduce our 2.5D grid representation in section 2. The process of terrain characterization is described in section 3. And a fuzzy logic-based traversability classifier is introduced in section 4. In section 5, experiments are studied comparing traversability assessment in our 2.5D grid-base maps and that directly form stereo data. Finally, a conclusion will be presented in section 6.

2. 2.5 Grid-based Map

Unlike navigation in indoor environment, the robot will have to consider diverse natural obstacles such as ramps and cliffs when operating in outdoor environment. For example, the robot must be able to use its map to identify and circumvent steep drops in elevations which might damage the robot while traversing more gentle elevation changes. In this case, the map must be capable of storing these features in order to provide the robot with the ability to determine the traversability of the anticipated areas. Conventional 2D occupancy grid will lack efficiency under this situation since the passablitiy of certain area often varies when estimated from different positions or orientations. The 3D grid map (Moravec, H. P. 1996 and Carsten, J. ; Ferguson, D. & Stentz, A. 2006) which extends the 2D grid map to a 3D array provides a closer approximation to outdoor environment. The number of grids in *Z* axis usually reflects the top (or average) height within the 2D grid patch. It is obvious that the resolution of the Z axis is especially important since it determines whether or not the robot can move from its current cell location to another cell. However, using an inappropriate resolution will make potential obstacle hidden in 3D grid map. For example, in Fig. 1, the maximum climbing height of an obstacle that robot can travel across is approximately 0.1 meters. If the difference in elevation of the next grid from the current one is greater than 0.1 meters, it should be considered as not traversable (obstacle). If we choose cell resolution height of 0.1 meters, the height of left cell is less than 0.1 meters, so number of the grids it occupies in Z axis is zero. Following the same principle we can tell that the right cell occupies one grid. In the 3D grid map, we find it possible to traverse between these two adjacent grids, while in fact, the elevation difference between the two cells is 0.11 meters, exceeding rover's maximum climbing height which is 0.1 meters. Therefore, the resolution height of 0.1 meters is not fine enough to detect obstacles. For two adjacent grid cells in 3D grid maps, let h_r be the real elevation difference value ; h_g be the elevation difference that the grids represent ; h_{max} be robot's maximum climbing height ; g be the size of one grid in Z axis. During the process of transforming the real elevation into grids, the maximun error

$$e_{\max} = \left| h_r - h_g \right| < 2g \,. \tag{1}$$

In this case, if we want to guarantee that the 3D grid map exists no hidden obstacle for robot, the gird size in Z axis

$$g < h_{\max} / 2 \,. \tag{2}$$

This conclusion shows that the resolution of height in 3D grid maps is highly associated with robot's climbing ability. However, mobile robots are not able to change their elevation as freely as aerial and underwater robots. The increase of resolution will heavily increase the cost of map maintanence.

Fong, E.H.L. et al (2003) and Gutmann, J.S. et al (2005) explore the development of a two and one-half dimemsional (2.5D) modeling method for autonomous mobile robot. The environment is represented by a regular 2D grid map of evenly spaced cells. Each cell holds the height of an obstacle or the floor covering the area at the cell's location (thus the term 2.5D). Phillipp, M. (2006) reconstructs 2.5D height map from online perception and utilize the map in navigation planning for biped robot. The 2.5D grid maps assign each grid cell a height value, or along with probability value, instead of dividing the *Z* axis evenly. This helps to make the robot operate safely by avoiding hidden obstacle in 3D grid map and decrease the cost of maintenance for storing the 3D grid array. If the 2.5D grid map is of high resolution, it can well represent surface profile like DEM (Digital Elevation Map). When resolution grows lower, the grids become more sparse and the map is inappropriate to describe continuous surface. So we attemp to extend the

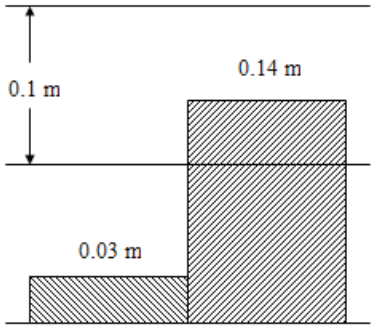

Fig. 1. Hidden obstacle caused by inappropriate resolution of Z axis

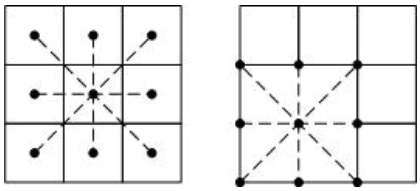

4. (b)

Fig. 2. (a) Graph extracted from Gutmann's 2.5D grid. (b) Graph extracted from our 2.5D Grid

2.5D grid for the outdoor or off-road environment, which is better to represent rough terrain surface.

The graph representing the Gutmann's 2.5D grid map can be extracted as illustrated in Fig. 2(a). Each grid can be represented by a node (black circle in Fig. 2(a)) which resides at the center of grid patch. The nodes are connected with edges (dashed line in Fig. 2(a)) for adjacent grid patches. Each node carries a height value (or along with probability value) which indicates the maximun/average height within the grid. Commonly, the grid size is set to be the minimum range that needed to envelop the robot regardless of its orientation and attitude. The graph extracted from our modified representation is showed in Fig. 2(b). Instead of grid centers, nodes reside at the corner of grid cells. Each node is assigned a height value indicating the average height within the grid. The edge between adjacent nodes records the traversability whether robot is able to travel from one to another. In our 2.5D grid map, the four corners of one grid actually indicate four adjacent nodes. By connecting adjacent nodes, we can form our DEM-like 2.5D grid-based map which is more similar with real terrain profile in off-road environment than that of Gutmann's. Addtionally, the grid size in our 2.5D grid map is set according to the wheel size of robot. The robot occupies multiple grids in the map during operation, which helps to provide a more rapid solution to terrain characterization and traversability assessment in the following sections.

3. Terrain Characterization

The result from stereo vision systems or LRF is a set of discrete three-dimensional points, each can be denoted as $\boldsymbol{p} = \begin{bmatrix} x & y & z \end{bmatrix}^T$ (where z is the height value). According to the x and y value, we can address the corresponding grid for every point p. For certain grid s_{ij}, the 3-dimensional points located in the same grid make up of point set $P_{ij} = \{p \mid x_{(i,j)} \le x < x_{(i+1,j)}, y_{(i,j)} \le y < y_{(i,j+1)}\}$, where $x_{(i,j)}$, $y_{(i,j)}$, $x_{(i+1,j)}$ and $y_{(i,j+1)}$ define the horizontal range of s_{ij}. Seraji, H. (1999) extracts slope and roughness from stereo vision information. As introduced in their work (Howard, A. & Seraji, H 2001), the slope is determined by the points located on the horizon line while the roughness is extracted by the size and concentration of detected rocks. This approach require the horizon line extracted and the rocks identified from the vision's feedback. Ye, Cang (2007) employs LDF, using slope and roughness to address the rraversability. The slope is determined by finding the least-square fit of P_{ij}, while the roughness is acquired as the residual of the best-plane fit. These two examples both extract terrain characteristics directly from dense point set that sensor returns. However, in our grid map, the grid size is determined by the size of robot's wheel, which makes the robot occupy several grids in the map. The assessment in our study looks at multiple nearby grids to determine the traversabiltiy instead of analyzing the dense point set P_{ij}.

Let S be the set of nodes which is extracted from the grid map, S_r represents the set of nodes which is to be assessed. For each grid s_{ij} belonging to S_r, let P_{ij} denote the point set located in the grid. Let n denote the number of points in P_{ij}. The average height h_{ij} of P_{ij} can be computed as

$$h_{ij} = \frac{1}{n}\sum_{i=1}^{n} z_i \text{ , for all point } p \in P_{ij} . \quad (3)$$

Terrain characteristics are rapidly assessed by analyzing heights of the grids belonging to S_r. Height difference defines the elevation difference between two grids. For specified grid s_i and its adjacent grid s_{i+1}, the height difference between the two grids can be calculated as

$$h_d = \left| h_{i+1} - h_i \right| . \quad (4)$$

Slope is an extremely relevant property as we do not want the rover going over large hills and alleys, as this increases its likelihood of the rover's tipping over, while roughness is the measurement of terrain's irregularity, which indicates the undulation frequency of terrain surface. We use the similiar method that Ye, Cang (2007) employs to address these two terrain properties. For the grids set S_r, we fit a plane to these patches in the sense of least-square error. The slope can be determined from the normal vector to the least-square plane which is denoted as $\boldsymbol{n} = \begin{bmatrix} n_x & n_y & n_z \end{bmatrix}^T$ and roughness is denoted by the residual of the fit $\sigma = \sqrt{\sum_{i=1}^{n} d_i}$, where d_i represents the distance between p_i and the fitting plane. As Ye, Cang (2004) & (2007) introduces in his research, the least-square plane is found by using the singular value decomposition (SVD) method (Golub, D.H. & Van Loan, C.F. 1986). First, the following n×3 matrix $\boldsymbol{A}$ is constructed using the height h_{ij} of each $s_{ij} \in S_r$:

$$\boldsymbol{A} = \begin{bmatrix} x_1 - \bar{x} & y_1 - \bar{y} & z_1 - \bar{z} \\ x_2 - \bar{x} & y_2 - \bar{y} & z_2 - \bar{z} \\ \vdots & \vdots & \vdots \\ x_n - \bar{x} & y_n - \bar{y} & z_n - \bar{z} \end{bmatrix}$$

where $\bar{x} = \frac{1}{n}\sum_{i=1}^{n} x_i$, $\bar{y} = \frac{1}{n}\sum_{i=1}^{n} y_i$ and $\bar{z} = \frac{1}{n}\sum_{i=1}^{n} z_i$.

Singular values σ_1, σ_2 and σ_3 ($\sigma_1 \geq \sigma_2 \geq \sigma_3 > 0$) of matrix $\boldsymbol{A}$ can be computed by means of SVD method. Then the eigenvalues λ_1, λ_2 and λ_3 of the 3×3 matrix $\boldsymbol{Q}$ ($\boldsymbol{Q}=\boldsymbol{A}^T\boldsymbol{A}$) and their corresponding eigenvectors are computed. It can be proven that the normal vector $\boldsymbol{n}=\left[n_x\ n_y\ n_z\right]^T$ to the least-square fit is equal to the eigenvector of matrix $\boldsymbol{Q}$ corresponding to $\lambda_{\min}=\min\left(\lambda_1,\lambda_2,\lambda_3\right)$ and the roughness which can be represented by the residual of the fit is

$$\sigma=\sqrt{\lambda_{\min}}\ . \tag{5}$$

With the normal vector of the best-plane fit, the slope of terrain that S_T represents can be estimated by

$$\varphi=\cos^{-1}\left(\boldsymbol{n}\cdot\boldsymbol{b}\right) \tag{6}$$

where $\boldsymbol{b}=\left(0,0,1\right)^T$ is the unit vector of z axis.

4. Fuzzy Logic-based Traversability Classifier

Height difference h_d, slope φ and roughness σ are the three terrain properties which we used to assess the traversability for robot. Fuzzy logic has been widely employed in the design of stable controller and is convenient to involve human knowledge by means of linguistic variables. The fuzzy logic-based traversability classifier inputs the terrain characteristics and output the linguistic traversability index. It performs three functions (Wang, L.X. 1997). First, fuzzification of the terrain characteristics is performed according to their corresponding membership functions (Fig. 3). Secondly, a fuzzy logic inference engine associates inputs to outputs based on a set of fuzzy logic rules. Finally defuzzification is performed according to the fuzzy membership function (Fig. 4) so as to generate the traversability index.

The fuzzy rules are concluded in Table 1. The empty entry in the table means the field has no influence on the index. These results are used to assess the traversability of terrain for the soccer robot which we employed in the following experiments.

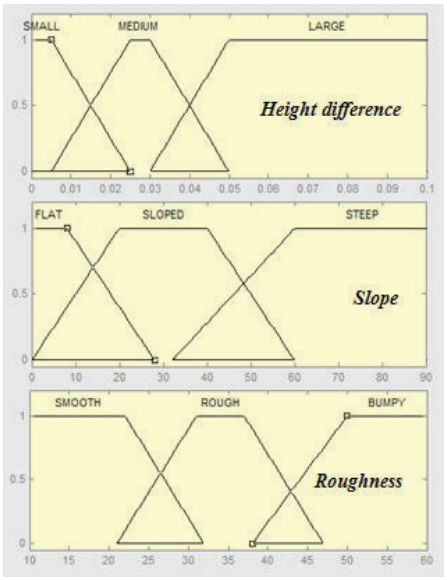

Fig. 3. Membership functions of inputs

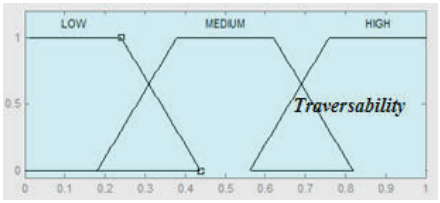

Fig. 4. Membership functions of output

Height difference	Slope	Roughness	Traversability index
SMALL	FLAT	SMOOTH	HIGH
SMALL	SLOPED	SMOOTH	HIGH
SMALL	FLAT	ROUGH	HIGH
MEDIUM	FLAT	SMOOTH	HIGH
LARGE			LOW
	STEEP		LOW
		BUMP	LOW
MEDIUM	SLOPED	ROUGH	LOW
MEDIUM	FLAT	ROUGH	MEDIUM
MEDIUM	SLOPED	SMOOTH	MEDIUM
SMALL	SLOPED	ROUGH	MEDIUM

Table 1. Fuzzy rules for traversability assessment

5. Experiment Results

Experiments are carried out to validate the correctness and efficiency of the traversability assessment employing our 2.5D grid map. A RoboCup soccer robot (Fig. 5), which employs a stereo vision system to perceive its circumstance, is used as a moblie platform in our experiments. The robot's length is about 50 centimeters and width is about 40 centimeters. The stereo vision system consists of two identical monochrome cameras with a distance (baseline) of 10 centimeters between them. The signal-to-noise ratio is about 50dB for each camera. The stereo vision is placed about 60 centimeters high from the ground with a angle of 30 degree towards the ground. It returns dense disparity points on the terrain surface through triangulation between left and right camera images. Each disparity point has three coordinate value indicating its position in space. The average heights of grids within the view of stereo vision are calculated from the set of disparity points as introduced in Equation (3).

Two sets of experiments are done in our study. The first set is that the robot assesses traversability indices directly from the disparity point returned by stereo vision. The other is that the indices are generated according to the corresponding grid sets of the area. The experiments employ disparity points within in the range of 4×4 square meters in front of robot. The size of grid is set to be 10×10 square centimeters.

Fig. 6 is the 2.5D grid map reconstructed from one pair of images from the stereo vision system. The disparity points are transformed into one uniform coordinate system after triangulation. The terrain characteristics can be calculated directly from the set of points or from our

Fig. 5. Outdoor experiments on terrain with elevation changes

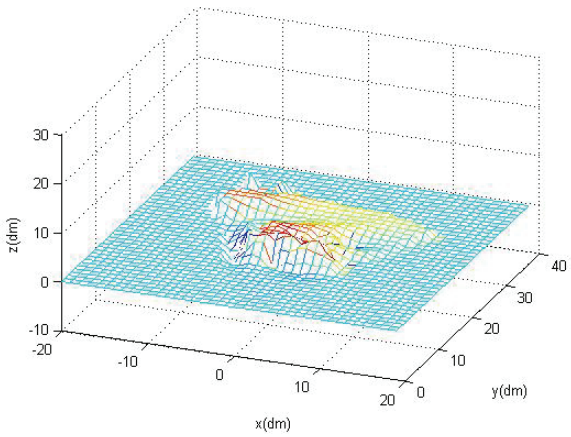

Fig. 6. 2.5D grid map reconstructed from a pair of stereo images.

2.5D grid after we update the 2.5D map according to these disparity points. We implement the two approaches and try to address the difference between the results from disparity points and those from our grids.

The ten values on the abscissa in Fig. 7 indicate the results of 10 experiments repectively. The solid line with star indicates the results directly calculated from the set of disparity points; the dashed line with square indicates the results acquired from the corresponding grid set. Fig. 7(a) illustrates that there are over 30,000 disparity points in the range of stereo vision system and they are distributed in about 1,000 grids. In Fig. 7(b), the green dashed line indicates the estimated real slope value of terrain within the range of 4×4 square meters in front of robot. The slope calculated directly from disparity points is influence by the noise of stereo vision system. The result from our structure is relatively closer to the real value of slope comparatively. The mean measurement adopted when calculating average height for each grid reduces the influence of noise in stereo perception. When finding the least-square fit, matrix $\boldsymbol{Q}$ involves more than 30,000 points if it directly works with the disparity set. Instead, by employing our grid structure, onlye about 1,000 grids are involved. In Fig. 7(c), we can see the time consumed to generate the slope is able to be saved by over 50%.

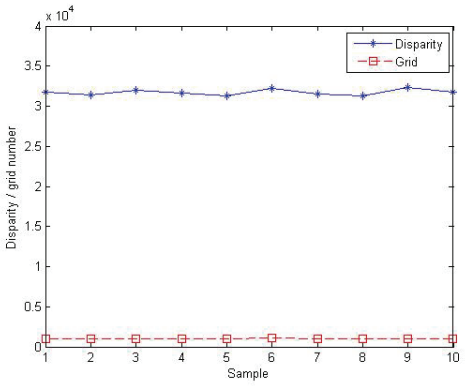

(a)

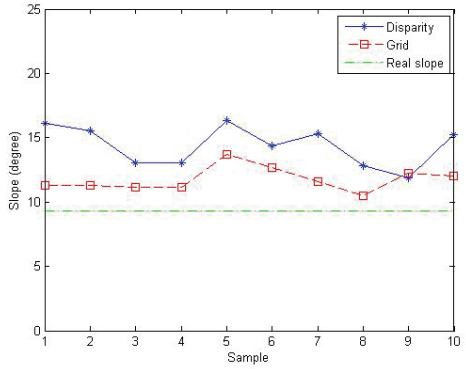

(b)

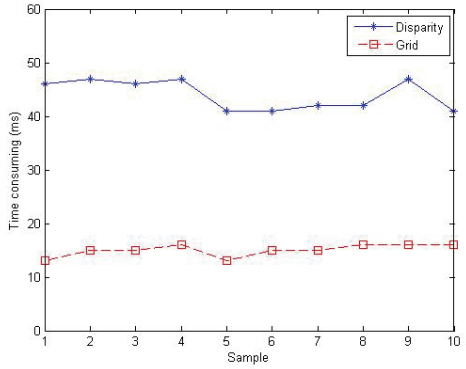

(c)

Fig. 7. Terrain characteristics extraction. (a) Number of disparity points and girds involved in calculation; (b) Extracted terrain characteristics of slope; (c) Time consuming of calculation.

When more disparity points are involved, the terrain assessment from our grids will become more efficient than that from disparity points. The experiments show that our 2.5D grid requires more cost of maintenance, but it will speed the traversability assessment and mildly reduce the influence of noise.

6. Conclusion

In this paper, we propose a rapid traversability assessment approach based on a 2.5D grid-based representaion of the rough terrain. For conventional grid-based maps, patch size is usually predefined as the minimum planar range which can fully envelop the robot

regardless of its attitude and orientation. When sensor systems like stereo are employed to perceive robot's surrounding circumstance, it takes time to generate terrain characteristics from the dense sensor data, which puts a constraint on the traversing speed of robot. Besides, potential path might be abandoned during planning because of the low resolution caused by the large grid size. Our approach tries to find a balance between the map resolution and the cost of map maintenance. The increased resolution of the map is also utilized to speed the process of traversability assessment by adopting our modified 2.5D grid structure. Experiment reslults show that our gird structure will save the time consumed to estimate traversability and provide a robust assessment result for the robot.

7. Reference

Carsten, J. ; Ferguson, D. & Stentz, A. (2006), 3D Field D*: Improved Path Planning and Replanning in Three Dimensions, Proceedings of IEEE/RSJ International Conference on Intelligent Robots and Systems (IROS), Beijing, pp.3381-3386 (2006)

Elfes, A. (1989), Using Occupancy Grids for Mobile Robot Perception, *Computer*, Vol. 22, No. 6, (6), pp.46-57, 0018-9162

Fong, E.H.L. ; Adams, W. ; Crabbe, F.L. & Schultz. A.C. (2003), Representing a 3-D environment with a 2 1/2-D map structure, Proceeding of IEEE/RSJ International Conference on Intelligent Robots and Systems (IROS), pp. 2986-2991, Oct., Las Vegas, Nevada

Golub, D.H. & Van Loan, C.F. (1986), Matrix Computations. Englewood Cliffs, NJ: Prentice-Hall, 1986.

Gutmann, J.S. ; Fukuchi, M. & Fujita, M. (2005), A floor and obstacle height map for 3D navigation of humanoid robot, Proceedings of IEEE International Conference on Robotics and Automation (ICRA), pp.1066-1071, Barcelona

Habib & Maki, K. (2007), Real time Mapping and dynamic navigation for mobile robots, *International Journal of Advanced Robotic Systems*, Vol. 4, No. 3, (9), pp. 323-338, 1729-8806

Hähnel, D. ; Burgard, W. & Thrun, S. (2003), Learning compact 3D models of indoor and outdoor environments with a mobile robot, *Robotics and Autonomous Systems*, Vol. 44, No. 1, (7), pp.15-27, 0921-8890

Howard, A. & Seraji, H (2001), Vision-based terrain characterization and traversability assessment, *Journal of Robotic Systems*, Vol. 18, No. 10, (9), pp. 577-587

Huang, G.Q. ; Rad, A.B. & Wong, Y.K. (2006). A new solution to map dynamic indoor environments, *International Journal of Advanced Robotic Systems*, Vol. 3, No. 2, (9), pp. 199-210, 1729-8806

Liu, H. ; Yang, J. & Zhao, C. (2004), A Generic Approach to Rugged Terrain Analysis Based on Fuzzy Interence, Proceedings of International Conference on Control, Automation, Robotics and Vision (ICARCV), pp. 1108-1113, Dec., Kunming

Moravec, H. P. (1996), Robot spatial perception by stereoscopic vision and 3D evidence grids. Technical Report CMU-RI-TR-96-34, CMU Robotics Institute, September 1996.

Murray, D. & Jennings, C. (1997), Stereo vision based mapping and navigation for mobile robots, Proceedings of IEEE International Conference on Robotics and Automation (ICRA), pp. 1694-1699, April

Phillipp, M. (2006), Online environment reconstruction for biped navigation, Proceedings of IEEE International Conference on Robotics and Automation (IRCA), pp. 3089-3094, 1050-4729, May, Orlando

Seraji, H. (1999), Traversability index: a new concept for planetary rovers, Proceedings of IEEE International Conference on Robotics and Automation (ICRA), pp 2006-2013, May, Detroit, Michigan

Shirkhodaie, A. ; Amrani R. ; & Tunstel, E. (2005), Soft Computing for Visual Terrain Perception and Traversability Assessment by Planetary Robotic Systems, Proceedings of IEEE International Conference on System, Man and Cybernetics, pp. 1848-1855, Oct.

Touchton, B. ; Galluzzo, T. ; Kent, D. ; & Crane, C. (2006). Perception and Planning Architechture for Autonomous Ground Vehicles, *Computer*, Vol. 39, No.12, (12), pp. 40-47, 0018-9162

Wang, L.X. (1997), *A Course in Fuzzy Systems and Control*, Prentice-Hall, 0-13-540882-2,

Ye, C. & Borenstein, J. (2004), A Method for Mobile Robot Navigation on Rough Terrain, Proceedings of IEEE International Conference on Robotics and Automation (ICRA), pp. 3863-3869, New Orleans

Ye, Cang (2007), Navigating a Mobile Robot by a Traversability Field Histogram, *IEEE Transactions on Systems, Man and Cybernetics*, Vol. 37, No. 2, (4), pp. 361-372, 1083-4419